Universiteit
Leiden
The Netherlands

Molecular electronics: controlled manipulation, noise and graphene architecture

Tewari, S.

Citation
Tewari, S. (2018, March 27). *Molecular electronics: controlled manipulation, noise and graphene architecture*. Casimir Research School, Delft. Retrieved from https://hdl.handle.net/1887/58611

Version:	Not Applicable (or Unknown)
License:	Licence agreement concerning inclusion of doctoral thesis in the Institutional Repository of the University of Leiden
Downloaded from:	https://hdl.handle.net/1887/58611

Note: To cite this publication please use the final published version (if applicable).

Cover Page

Universiteit Leiden

The following handle holds various files of this Leiden University dissertation:
http://hdl.handle.net/1887/58611

Author: Tewari, S.
Title: Molecular electronics: controlled manipulation, noise and graphene architecture
Issue Date: 2018-03-27

1. Introduction

Greek and Indian philosophers were the first to give an atomic theory of matter. In their description, the atom, the smallest constituent of the matter was indestructible. However, we know now that the atoms are more than willing to share a part of them, i. e. electrons. In fact, by sharing these electrons, atoms form molecules, which consequently form the matter. Hence, by philosophying the atom as indestructible, the very existence of matter was dismissed. Furthermore, the flow of these electrons in matter is what gives current. It is fascinating to observe that it is now routinely possible to wire an organic molecule, an object as small as one nanometer, between two metallic leads and measure its electronic transport characteristics. In parallel, many theoretical tools have been developed and refined for describing such transport properties and for obtaining numerical predictions. The theoretically predicted trends nowadays reproduce the experimental findings quite well for series of molecules with a single well-defined control parameter, such as the length of the molecules. The quantitative agreement between theory and experiment usually is less convincing, however. Many reasons for quantitative discrepancies can be identified, from which one may decide that qualitative agreement is the best one may expect with present modeling tools. For further progress, benchmark systems are required that are sufficiently well-defined by experiment to allow a quantitative testing of the approximation schemes underlying the theoretical modeling.

1.1 The concept of the atom

Greek philosopher Leucippus (with his disciple Democritus) and Indian philosopher Kanada were the first to give an atomic theory of matter[1]. In their description, the atom, the smallest constituent of the matter was indestructible. It only became clear in early 20th century, by the work of Thomson[2], Lewis[3] and Langmuir[4] that atoms join together by sharing a part of them i. e. electrons, to form molecules.

Next, came the development of quantum mechanics, which changes the way we imagine the fundamental particles. A core concept of quantum mechanics is the wave nature of electrons postulated by Louise de Broglie[5] in 1929. Soon after, Schrödinger gave a differential wave equation, known as the Schrödinger equation to study quantum mechanical systems. This gave birth to the notion of the wavefunction. Consequently, this picture of a wavefunction had many implications. What followed were partially counterintuitive and exotic phenomena like quantum tunnelling, Heisenberg uncertainty principle, quantum superposition, quantum interference etc.

Researchers from IBM utilised the phenomenon of quantum tunnelling to image single atoms and molecule. They invented[6,7] in 1981; the machine called the scanning tunnelling microscope (STM), which makes use of the fact that the electron wave functions extend in space out of their parent atom in an exponentially decreasing fashion. After the advent of STM, it became possible to image conducting surfaces with atomic resolution. STM operates by bringing the apex of a fine metallic wire into tunnelling distance from a surface of interest. By providing feedback in the tunnel current and scanning the tip above the surface, one can make topographic maps of the surface with atomic resolution. STM has found its applications in many fields of science. Apart from studying surface topography, STM has been used for manipulating single atoms[8–10], for doing spectroscopy[11], for fabricating nano-structures with new tweaked electronic properties[12], for studying surface chemistry[13], for probing collective[14] and local[15] electronic behavior, and much more.

[1] R. A. Horne. In: *Ambix* 8 (1960), p. 98.
[2] Sir J. J. Thomson O.M. F.R.S. In: *The London, Edinburgh, and Dublin Philosophical Magazine and Journal of Science* 27 (1914), p. 757.
[3] Gilbert N. Lewis. In: *Journal of the American Chemical Society* 38 (1916), p. 762.
[4] Irving Langmuir. In: *Journal of the Franklin Institute* 187 (1919), p. 359.
[5] Louis De Broglie. PhD thesis. Migration-université en cours d'affectation, 1924.
[6] Gerd Binnig et al. In: *Phys. Rev. Lett.* 49 (1982), p. 57.
[7] Gerd Binnig and Heinrich Rohrer. In: *Rev. Mod. Phys.* 59 (1987), p. 615.
[8] Donald M. Eigler and Erhard K. Schweizer. In: *Nature* 344 (1990), p. 524.
[9] Joseph A. Stroscio and D. M. Eigler. In: *Science* 254 (1991), p. 1319.
[10] Saw Wai Hla. In: *Reports on Progress in Physics* 77 (2014), p. 056502.
[11] R. Wiesendanger. Scanning Probe Microscopy and Spectroscopy: Methods and Applications. Cambridge University Press, 1994.
[12] H. C. Manoharan et al. In: *Nature* 403 (2000), p. 512.
[13] Joost W. M. Frenken and Irene Groot. Vol. 114. Operando research in heterogeneous catalysis. Springer, 2017.
[14] Hanno H. Weitering et al. In: *Science* 285 (1999), p. 2107.
[15] S. H. Pan et al. In: *Nature* 403 (2000), p. 746.

1.2 From macro to nano

As the nanoscale dimensions became accessible, it became a hot topic to understand how electronic transport occurs in such nanoscale devices. Molecular electronics is an approach to study nano-electronics on the scale of single atoms and molecules. From Ohm's law, we know that conductance scales with the area of the macroscopic conductor: $G = \sigma \frac{A}{l}$, where A is area and l is the length of the macroscopic wire. Based on dimensions of the system, electronic transport can be divided into two regimes: diffusive and ballistic. When the size of the system is larger than the mean free path[1] of an electron, then the electron loses part of its momentum to other electrons and atoms in the lattice before crossing the system. Such transport is called diffusive transport. Maxwell gave an expression for conductance of a point contact in such diffusive regime[16] as $G = 2\sigma R$, where R is the radius of the cross-section of the contact.

On the contrary, when the size of the system shrinks below the mean free path of the electrons, then the electron crosses the system ballistically without losing its momentum. This regime is thus called the ballistic regime. Sharvin in 1965[17], showed that the conduction electrons passing through an orifice (in a ballistic manner) should change their velocity by an amount $\Delta v \approx eV/p_F$, where eV is the potential drop across the orifice, and p_F is the Fermi momentum. From this, the Sharvin conductance for the ballistic contact can be derived as:

$$G = \frac{2e^2}{h}\left(\frac{k_F R}{2}\right)^2 \tag{1.1}$$

Which is directly proportional to R^2 but it is independent of the length of the conductor. Here $k_F (= p_F/\hbar)$ is the Fermi wave-vector. The Heisenberg uncertainty principle for Fermi electrons in a narrow-contact, $2p_F R \geq \hbar$ gives a small correction (called Weyl correction)[18] to the Sharvin conductance:

$$G = \frac{2e^2}{h}\left(\frac{k_F R}{2}\right)^2 \left(1 - \frac{2}{k_F R} + ...\right) \tag{1.2}$$

This equation is now valid for a contact down to a few nanometers in diameter (in the form of wire, not orifice) and is often used to establish the relationship between the conductance and the radius of a contact.

When the size of the contact becomes so small that the wave-nature of an electron can no longer be ignored and the quantum mechanics has to come in, then the correct expression for the conductance is given by Landauer (for low-bias regime) as[2]:

[1] Mean free path is the distance an electron can move in a medium without losing its momentum.

[2] The expression given here is for spin degenerate systems. For spin split systems, the expression becomes: $G = \frac{e^2}{h} \sum T_n$.

[16] Juan Carlos Cuevas and Elke Scheer. Molecular electronics : an introduction to theory and experiment. New Jersey [u.a.] : World Scientific, 2010.

[17] Yu V. Sharvin. In: *J. Exptl. Theoret. Phys. (U.S.S.R.)* 48 (1965), p. 655.

[18] Nicolás Agraït et al. In: *Physics Reports* 377 (2003), p. 81.

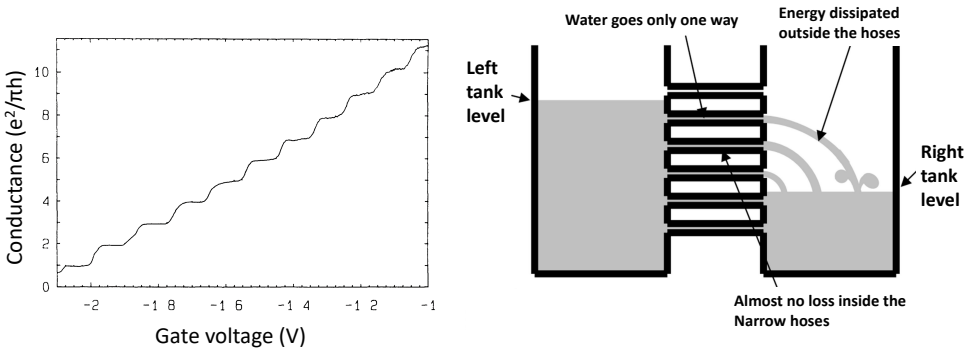

(a) (b)

Figure 1.1: (a) Conductance quantization measured in a 2DEG system by van Wees *et al*.[20](b) A pictorial explanation of conductance quantization from the book by Ouisse[21].

$$G = \frac{2e^2}{h} \sum_{n=1}^{N} T_n \tag{1.3}$$

Here, conductance is directly proportional to sum over transmission through different channels (given by index n). In a metallic conductor of cross-section area A, the total number of independent transmission channels N is given by A/λ_F^2, where λ_F is the Fermi wavelength[19]3. Such conductance quantisation was measured experimentally by van Wees *et al*.[20] in 1988 in a two-dimensional electron gas (2DEG) system. With the help of a gate electrode, the researchers were able to start from a completely pinched off regime and controllably open channels one after the other measuring step-wise increase in conductance as shown in Figure 1.1(a). Figure 1.1(b) shows a pictorial analogy of the conductance quantisation to a water tank experiment (taken from the book by Ouisse[21]). In the picture, the two parts of a water tank are separated by a series of water channels. The water level on left and right side depicts the Fermi level of electrons on the left and right leads connecting to the point contact. As the water level (Fermi level) rises on one side of the tank (leads), more and more water channels (electronic transport channel) are opened and thus increasing the total flow of water (total conductance) from left to right reservoirs.

Soon after, such conductance quantization was observed also in a three dimensional metallic point contacts by Krans *et al*.[22,23] in 1993. They measured it using

3 Fermi-wavelength in bulk gold is around 0.5 nm.

[19] C. W. J. Beenakker, Christian Schönenberger, et al. In: *Physics Today* 56 (2003), p. 37.
[20] B. J. van Wees et al. In: *Phys. Rev. Lett.* 60 (1988), p. 848.
[21] Thierry Ouisse. Electron transport in nanostructures and mesoscopic devices: an introduction. John Wiley & Sons, 2013.
[22] J. M. Krans et al. In: *Phys. Rev. B* 48 (1993), p. 14721.
[23] C. J. Muller et al. In: *Phys. Rev. B* 53 (1996), p. 1022.

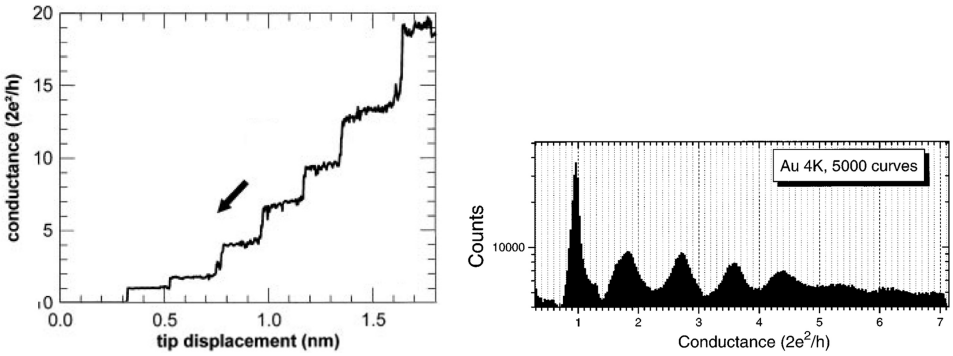

(a) (b)

Figure 1.2: (a) Conductance steps associated quantization measured in a gold (Au) point contact (b) A typical conductance histogram of Au atomic point contacts. Above Figures are taken from Rubio *et al*.[24] and Costa-Krämer *et al*.[25]

a mechanically controlled break junction technique to controllably break and form single atom contacts. Due to complex dynamics of these metallic systems, a large conductance data-set is often recorded for different contact configurations and a conductance histogram is prepared. Figure 1.2 shows an example of such conductance quantization and histogram taken from Rubio *et al*.[24] and Costa-Krämer *et al*.[25]. The step-wise conductance in this case is a result of a combination of conductance quantization and discrete atomic configurations.

1.3 Molecular electronics

Molecular electronics is like a Utopian[4] dream for future electronic circuits where molecules will become the building blocks. Here, the electronic components based on silicon technology will be replaced by single molecules with similar and even more functionalities. Switches made from single molecules will give an exceptionally high switching rates and clock frequency, increasing the computational power of the current circuits by manifolds. These molecules will convert heat and light to electricity far more efficiently than current technology. Not to forget the small molecules will bring with them pleasant surprises using their quantum mechanical properties even at room temperature. In spite of all this and many more benefits, the power consumption of these circuits will be significantly smaller than current circuits due to less heat loss and efficient electron transfer.

This led researchers from different fields (experimental physics, theoretical physics, synthetic chemistry, biology and industries) to come together and work for the realization of such a dream. A lot has been done starting from connecting single molecules between metallic leads, studying their mechanical and electronic transport properties, their quantum mechanical behaviours and so on. Einstein said once, *"As our*

[4] Utopian in terms of idealistic but not impossible.

[24] G. Rubio et al. In: *Phys. Rev. Lett.* 76 (1996), p. 2302.
[25] J. L. Costa-Krämer et al. In: *Phys. Rev. B* 55 (1997), p. 12910.

circle of knowledge expands, so does the circumference of darkness surrounding it." that is, the more we will know the more of the unknown will be visible. In fact, this is also the current situation with molecular electronics, there are many things we have learned so far but many still to be understood and put under control from both fundamental and technological point of view.

Now that we understand and control the basic properties of molecular junctions the time is ripe to critically evaluate the question how well we understand electron transport in molecular junctions. Theory inevitably needs to take into account many details of the arrangements of the atoms and the molecule that make up the junction. Since self-assembly is an essential element in the formation of molecular junctions and imaging of the resulting structures has not been possible, experiment usually does not provide all the information needed for comparison with theory. The problem that we want to address arises largely because of a want for suitable benchmark systems that have been sufficiently characterized by experiment such that they may be used for a critical evaluation of the theories. The problem is the more important since interpretation of the experiments often heavily relies on a comparison with model calculations.

Despite many experimental hurdles the understanding of electron transport of single-molecule junctions has seen impressive progress in recent years[16]. It is fascinating to observe that it is now routinely possible to wire an organic molecule, an object as small as one nanometer, between two metallic leads and measure its electronic transport characteristics. Several approaches even allow bringing a third metal lead close enough to serve as a gate electrode, through which the conductance of the molecule can be adjusted electrostatically.

1.4 Experimental techniques

In this section we briefly present various techniques used for studying electronic transport through single molecules. For a more detailed presentation of single-molecule techniques and their integration into various advanced measurement schemes we refer to following reviews[18,26–28]. Since molecules have a typical size of 1 nm all existing top-down microfabrication techniques lack the required resolution for controlled wiring of molecules. Therefore, the methods employed rely on a combination of electromechanical fine tuning of the nanometer-size gap between the contact electrodes and self-assembly of the molecules inside this gap. The three most frequently employed techniques are the mechanically controlled break junction (MCBJ) technique, the electromigration break junction (EBJ) technique and methods using scanning tunneling microscopes (STM).

1.4.1 Mechanically controllable break junctions

The MCBJ technique was developed for the study of atomic and molecular junctions[29] based on an earlier method which aimed at studying vacuum tunneling between

[26] Dong Xiang et al. In: *Advanced Materials* 25 (2013), p. 4845.
[27] Dong Xiang et al. In: *Chemical Reviews* 116 (2016), p. 4318.
[28] Sriharsha V. Aradhya and Latha Venkataraman. In: *Nature Nanotechnology* 8 (2013), p. 399.
[29] C. J. Muller et al. In: *Physica C: Superconductivity* 191 (1992), p. 485.

superconductors.[30] We distinguish two fabrication methods: the notched-wire MCBJ, and the lithographically fabricated MCBJ. The first is the simplest and has the advantage that it can be easily adapted to nearly all metal electrodes. It is made starting from a macroscopic metal wire into which a weak spot is created by cutting a notch. The notched metal wire is placed on top of a flexible substrate (which is commonly stainless steel or phosphorous bronze) covered by an insulating sheet, usually Kapton. The wire is fixed by epoxy onto the substrate at either side and very close to the notch. This is then mounted in a three-point bending mechanism as shown in Figure 1.3(a), where the flexible substrate is held down at the two ends and pushed up in the middle. Bending the substrate increases the strain in the wire, which is concentrated at the weak spot created by the notch, until the wire breaks. The junction is first broken with a coarse mechanical drive, thus exposing two fresh electrode surfaces. By relaxing the bending and using fine control of the separation gap by means of a piezo-electric actuator atomic-size contacts can be reformed and broken many times.

The lithographically fabricated MCBJ[31] (shown in Figure 1.3(b)) shares the same principle as the notched-wire MCBJ except that the pre-notched metal wire is replaced by a freely-suspended bridge in a thin metal film produced by electron-beam lithography. This metal film is electrically isolated from the flexible substrate using a $3-5\ \mu$m polyimide layer. The unsupported section of the bridge is reduced by about two orders of magnitude compared to the notched-wire MCBJ to about $2\ \mu$m. This has the effect that the mechanical displacement ratio, i. e. the ratio between the change of the gap size and the actuator motion, is reduced to about 1×10^{-5}. The gain of the lithographic technique is that the junctions are very insensitive to external mechanical perturbations as a result of the small displacement ratio. The added complications of clean-room preparation are offset by the possibility of producing multiple MCBJ samples on a single wafer[32]. A drawback is the fact that by the very small displacement ratio the maximum extension of a typical piezo actuator produces less than 0.01 nm change in the distance between the electrodes. Therefore, the control of this distance is achieved by an electro motor driven gear. Since such electromechanical control is much slower than piezo-electrical control it is much more time consuming to obtain enough statistics for a large number of contact breaking events (see below).

For most types of metal electrodes one can only take full advantage of the MCBJ method by performing the first breaking at cryogenic temperatures or under ultra-high vacuum (UHV). Otherwise, the surfaces will be contaminated with oxides and adsorbents will cover the surface within a fraction of a second, so that the atomic-size contact characteristics of the pure metal are lost. The main exception is Au[33], for which even under ambient conditions most of the intrinsic quantum conductance properties survive as a result of the low reactivity of the Au surface[34].

For the same reason Au stands out as the preferred electrode material for all other single-molecule transport experiments. Specific binding to target molecules can be achieved by selecting suitable anchor groups for the molecules. Sulfur

[30] John Moreland et al. In: *Applied Physics Letters* 43 (1983), p. 387.
[31] J. M. van Ruitenbeek et al. In: *Review of Scientific Instruments* 67 (1996), p. 108.
[32] Christian A Martin et al. In: *New Journal of Physics* 10 (2008), p. 065008.
[33] B. Hammer and J. K. Norskov. In: *Nature* 376 (1995), p. 238.
[34] J. I. Pascual et al. In: *Phys. Rev. Lett.* 71 (1993), p. 1852.

groups are widely exploited for this purpose, but several other possibilities have been explored[35]. Typically, such molecules having suitable anchor groups are deposited onto the bridge of the MCBJ from solution, under ambient conditions. This has been first explored for lithographic MCBJ systems[36], and this continues to be the most commonly employed approach. A few groups[37–39] though also work with notched-wire MCBJ technique for connecting single molecules and have recently demonstrated sharp conductance histogram measurements over an oligo phenylene-ethynylene (OPE-3) molecule[39].

The intrinsic cleanliness of the broken metal surfaces can be fully exploited by working under UHV and/or under cryogenic conditions. The deposition of molecules in these experiments proceeds by deposition onto the broken junction from the gas phase, either using an external vapor source[40,41] or employing a local cell for sublimation[42,43]. By working under cryogenic or under UHV conditions it is possible to explore other metal electrodes and other forms of metal-molecule bonding. For example, hydrogen, H_2, binds to clean Pt electrodes without the need for anchoring groups[40], and this applies more widely also for many organic molecules such as benzene[41], oligoacenes[44] and pyrazene[42].

1.4.2 Electromigration break junctions

Electromigration in metals[45] results from an atom diffusion process driven by the 'electron wind' force[46] exerted by the conducting electrons on the atoms in the system, under large current bias. This effect can be used to create nanogaps in metallic leads[47,48], small enough for a single molecule to bridge. Such systems are prepared by first pre-patterning a narrow metal wire of about 100 nm in a thin metallic film on an insulating substrate (usually SiO_2 on a Si wafer) using electron lithography. Passing a large current through such narrow metallic leads gives rise to displacement of atoms, which is observed as an increasing resistance due to the gradual opening of a gap in the narrow wire. Initially the reliability of the method was compromised by the fact that the strong local Joule heating leads to the formation of metallic nanoparticles in almost 30% of the junctions[48,49], which give rise to characteristics resembling those of molecules. However, by using a feedback circuit the electromigration process can

[35] Chuancheng Jia and Xuefeng Guo. In: *Chem. Soc. Rev.* 42 (2013), p. 5642.
[36] J. Reichert et al. In: *Phys. Rev. Lett.* 88 (2002), p. 176804.
[37] M. Kiguchi et al. In: *Journal of Physics: Conference Series* 100 (2008), p. 052059.
[38] T. Yelin et al. In: *Nano letters* 13 (2013), p. 1956.
[39] Julian M. Bopp et al. In: *Low Temperature Physics* 43 (2017), p. 905.
[40] R. H. M. Smit et al. In: *Nature* 419 (2002), p. 906.
[41] M. Kiguchi et al. In: *Phys. Rev. Lett.* 101 (2008), p. 046801.
[42] Satoshi Kaneko et al. In: *Nanotechnology* 24 (2013), p. 315201.
[43] D. Rakhmilevitch et al. In: *Phys. Rev. Lett.* 113 (2014), p. 236603.
[44] T. Yelin et al. In: *Nature materials* 15 (2016), p. 444.
[45] P. S. Ho and T. Kwok. In: *Reports on Progress in Physics* 52 (1989), p. 301.
[46] H. B. Huntington and A. R. Grone. In: *Journal of Physics and Chemistry of Solids* 20 (1961), p. 76.
[47] Hongkun Park et al. In: *Applied Physics Letters* 75 (1999), p. 301.
[48] Herre S. J. van der Zant et al. In: *Faraday Discuss.* 131 (2006), p. 347.
[49] A. A. Houck et al. In: *Nano Letters* 5 (2005), p. 1685.

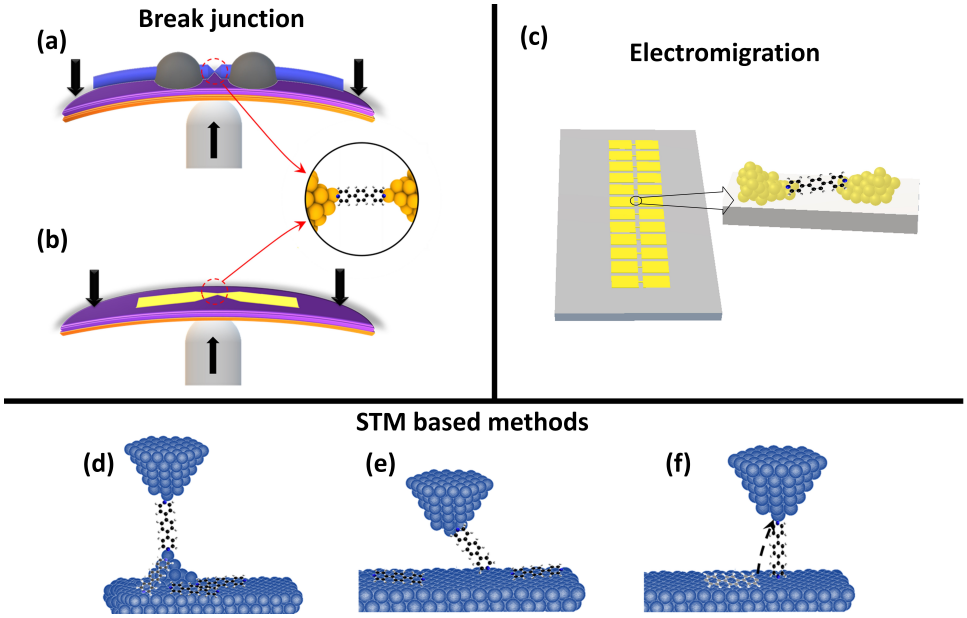

Figure 1.3: Overview of experimental techniques aimed at measuring single-molecule transport. (a) Notched-wire MCBJ mounted in a 3-point bending configuration and wire is anchored to the substrate with black stycast epoxy, (b) Lithographically prepared gold MCBJ mounted also in 3-point bending configuration, (c) Electromigration based junctions where the size of gap is not adjusted to the size of the molecule as shown in the blown up picture of the junction, (d) STM break junction setup, where after a few indentation cycles the atomic configuration of the electrode on the surface side becomes unknown, (e) I(t) and I(s) technique done at room temperature in STM where the tip is not indented on the surface and (f) Recent developments in controlled formation of single molecule junctions using low temperature UHV systems.

be more precisely controlled, and further improvements are obtained by relying on self-breaking in the last stages of gap formation[50]. A schematic is shown in Figure 1.3(c).

Molecules are deposited onto the nanowire before electromigration, and one relies on a molecule finding its way to the gap during the electromigration process. Alternatively, molecules can be allowed to self-assemble into the gap from solution after the electromigration process has been completed[51]. In contrast to the other break junction techniques, junctions formed by electromigration can only be broken once and cannot be reformed. The gap distance depends on the details of the feedback breaking process, but it cannot be targeted very precisely. One cannot obtain a very precise value for the size of the gap, but a fair estimate can be obtained from fitting the IV characteristics to the Simmons model[52,53]. For imaging techniques the gap

[50] K. O'Neill et al. In: *Applied Physics Letters* 90 (2007), p. 133109.
[51] Edgar A. Osorio et al. In: *Nano Letters* 7 (2007), p. 3336.
[52] John G. Simmons. In: *Journal of Applied Physics* 34 (1963), p. 1793.
[53] Ayelet Vilan. In: *The Journal of Physical Chemistry C* 111 (2007), p. 4431.

is better accessible than any of the other techniques discussed here. High-resolution transmission electron microscopy imaging using transparent SiN_x membranes was done for gold electromigration junctions[54,55] for stuying the breaking process and detecting the nanogap size. Due to the three dimensional shape of leads it is difficult to obtain precise values for the gap. The imaging resolution of transmission electron microscopy has not yet proven sufficient for detecting the position of an organic molecule.

The search for junctions bridged by a molecule is based on producing many (of order several hundred) electromigration break junctions on a wafer, breaking each of them separately, and scanning the resulting junctions for interesting IV characteristics at room temperature, that may point at the presence of a molecule in the bridge. Such junctions, which are a minority of order a few percent, are then further studied, usually by more elaborate techniques. Although the method intrinsically permits very limited statistics over molecular junction configurations, and every junction formed has its particular characteristics, the more elaborate experiments make very interesting case studies. Moreover, the rigid attachment of the electrodes to the substrate allows temperature and field cycling, it allows the fabrication of a metallic gate at close proximity to the junction[47,48], and it permits easy optical access for Raman scattering[56]. Such experiments provide evidence for the presence of the molecule in the junction by giving exquisitely detailed excitation spectra of vibrations in inelastic tunneling[51], in the simultaneously detected Raman spectrum[56,57], and of magnetic excitations in the differential conductance[58].

1.4.3 Methods based on scanning probe microscopy

The break junction methods described above do not permit imaging of the molecule in the junction. In contrast, scanning tunneling microscope (STM) or atomic force microscope allow imaging molecules on a surface before contacting them. This is possible only for very stable systems under UHV and at cryogenic temperatures[59,60]. By imaging and manipulating single molecules on an atomically flat and clean metal surface it is possible to verify that the STM tip interacts with a single target molecule and the shape of the bottom electrode contacting the molecule (the metal surface) is known. However, information on the shape of the tip cannot be easily obtained from experiments. Moreover, when approaching the tip for contacting the molecule and lifting it up from the surface the molecule and the metal atoms contacting it rearrange in ways that cannot be seen by the instrument. In Chapter 3, we will discuss further in more detail on such techniques. A schematic showing controlled manipulation is given in Figure 1.3(f).

While cryogenic UHV STM holds great promise, it is also a very demanding technique. A very powerful and versatile method for investigating the conductance of single molecules at room temperature and in solution was introduced by Xu *et*

[54] Douglas R. Strachan et al. In: *Phys. Rev. Lett.* 100 (2008), p. 056805.
[55] B. Gao et al. In: *Nanotechnology* 20 (2009), p. 415207.
[56] Daniel R. Ward et al. In: *Nano Letters* 8 (2008), p. 919.
[57] Madoka Iwane et al. In: *Sensors* 17 (2017), p. 1901.
[58] R. Gaudenzi et al. In: *The Journal of Chemical Physics* 146 (2017), p. 092330.
[59] R. Temirov et al. In: *Nanotechnology* 19 (2008), p. 065401.
[60] Torben Jasper-Tönnies et al. In: *Phys. Rev. Lett.* 119 (2017), p. 066801.

al.[61] (schematic shown in Figure 1.3(d)), which has inspired many other researchers. Ignoring the scanning capability of STM, the instrument is used for approaching the tip to the surface and repeatedly indenting the tip into the surface and retracting. This resembles closely the MCBJ type of experiments, with the added advantage that it permits simple adaptations for operating in a solution of the target molecules. The indentation of the (Au) tip into the (Au) metal surface to a depth corresponding to a conductance of 10–40 times the conductance quantum ($G_0 = 2e^2/h$) restructures the shape of the electrodes with every indentation. Upon retraction a neck is formed that thins down until it snaps. The resulting gap is then frequently bridged by a molecule equipped with suitable anchoring groups through a self-organization process, which is observed as a plateau in the conductance during retraction. These plateaus usually have a lot of structure and appear at different levels for each retraction event. Therefore, the indentation and retraction cycles are repeated many times and the resulting conductance traces are then combined in form of conductance histograms, as had been previously introduced for MCBJ experiments[22,40].

Using a conducting probe AFM one can simultaneously measure both the conductance and force between the tip and the molecule[28,61]. These room temperature experiments have the great advantage that they permit evaluating single-molecule junctions much faster than the other available techniques, and thereby allow exploring trends as a function of molecular composition.

1.4.4 Data analysis and conductance histograms

Most of the MCBJ and STM experiments have in common that, as a result of the self-organization process involved in the formation of the junction, very little is known about the atomic-scale shape and structure of the electrodes, about the configuration of the molecule in the junction, and about its bonds to the metal surfaces. The effect of these parameters on the conductance is observed as a variation, usually by about an order of magnitude or more, in the observed conductance between independent realizations of molecular junctions. The solution that is widely adopted is to repeatedly form and break many junctions, record the digitized conductance during the contact breaking process, and collect all data in a histogram. The underlying assumption is that sufficiently deep indentation restructures the metal leads and the molecule, and randomizes the path followed in configuration space during the contact breaking process. The peaks in the histogram can then be interpreted as representing the energetically favorable junction configurations, and these are the most relevant parameters used for comparison with model calculations. By combining the displacement length measured from the point of metal-metal contact breaking with the evolution of the conductance one can also build two-dimensional histograms[32], which are helpful for detecting multiple stable configurations and for obtaining a measure of the molecular bridge length.

In the breaking process the last-atom metal-to-metal contact is usually clearly visible as a plateau near 1 G_0, and this produces a sharp peak in the conductance histogram. Breaking of this last metal contact is followed by a jump out of contact[62] to a conductance that is one or two orders of magnitude lower. In many cases, after this jump the current exponentially decreases with increasing separation of the electrodes,

[61] Bingqian Xu and Nongjian J. Tao. In: *Science* 301 (2003), p. 1221.
[62] N. Agraït et al. In: *Phys. Rev. B* 47 (1993), p. 12345.

as expected for vacuum tunneling. Only for a fraction of the breaking events one or more plateaus appear signaling the bridging by a molecule. The large number of traces without a molecular signal results in a large background in the histograms. Initially, curves without a clear molecular signature were manually removed from the data set. This practice has some danger of introducing experimenter-bias in the data selection, and this practice has now been abandoned. The background problem can be reduced by the use of automated routines, for example routines that detect the last step in the conductance[63]. Other solutions proposed include the application of an AC modulation of the gap distance[64]. A widely adopted solution to the background problem uses histograms of the logarithm of conductance, rather than the linear conductance[65]. In this case the background tunneling contribution reduces to a nearly constant contribution and the relevant features related to the molecule will be more clearly visible in a data-set that now comprises all breaking traces.

The appearance of the shape of the histograms and the positions of the peaks for the same metal-molecule system do not reproduce perfectly between experimental groups, and even from one experimental run to the next. This implies that the underlying assumption that the repeated indentation effectively averages over all configurations is not fully justified. For example, one may anticipate that the results will be sensitive to parameters such as the voltage or current bias applied, and the depth of indentation. This has motivated Haiss *et al*. to avoid indenting the surface, in order to maintain a common surface and tip structure. They developed the so-called I(t) and I(s) techniques[66,67] shown in Figure 1.3(e). These techniques operate near room temperature and rely on bringing the STM tip close to the surface by the usual current feedback control. For low surface coverage molecules with suitable anchoring groups are expected to jump stochastically into and out of contact with the tip. The difference between I(s) and I(t) is that the tip is moved in and out of close distance to the surface repeatedly for the former, while in the latter case, the tip is held at a stable tunneling distance and the events are recorded as a function of time. The conductance values measured by I(t) or I(s) are found to be up to an order of magnitude smaller than the ones obtained from histograms produced by MCBJ or STM techniques.

1.5 The notorious lot

Apart from the interesting work that has been done so far in single-molecule transport measurements and the new important physics that has been probed in these systems, there is still a "notorious lot" which needs to be highlighted and not put under the carpet. Thiol (-SH) anchoring group and gold electrode make a congruous combination for doing single-molecule electronics. This combination has been used since researchers started to study self-assembled mono-layers of molecules. It is still heavily used for anchoring various single-molecules between gold electrodes. However, some simple key dithiol molecules that have been studied by many group

[63] Sung-Yeon Jang et al. In: *Nano Letters* 6 (2006), p. 2362.
[64] J. L. Xia et al. In: *Nano Letters* 8 (2008), p. 1960.
[65] M. Teresa González et al. In: *Nano Letters* 6 (2006), p. 2238.
[66] Wolfgang Haiss et al. In: *Journal of the American Chemical Society* 125 (2003), p. 15294.
[67] Wolfgang Haiss et al. In: *Phys. Chem. Chem. Phys.* 6 (2004), p. 4330.

in early 21^{st} century, have shown a large spread (over few orders of magnitude) in their conductance values. This include the famous Benzenedithiol molecule and the family of Alkane dithiols. I will give a brief review of these two sets because they clearly illustrate the need for more advanced techniques, to which the rest of this thesis is devoted.

1.5.1 Benzenedithiol

The first electronic transport measurement over a single molecule dates back to 1997 by Reed *et al*.[68], where a benzene-1,4-dithiol molecule was measured between two gold electrodes. A benzene-1,4-dithiol molecule sandwiched between two gold leads forms 1,4 benzene-dithiolate (BDT) after the two hydrogen atoms are lost from the sulfurs. The benzene ring provides the π electrons for conduction, and the sulfur is supposed to bind in a covalent manner to the gold leads. The conductance measurement done over the molecule has shown a conductance gap of around 0.7 V which was attributed to a gap between the leads Fermi level and the lowest unoccupied molecular orbital (LUMO) of the molecule. At positive and negative bias the conductance is shown to rise in a step manner with the first plateau around 2 V having a value of 45 nS (or 5.8×10^{-5} G_0). This is considered as the characteristic conductance of the BDT molecule. Followed by this several theoretical models were proposed[69–72] to understand the above experimental result, but surprisingly the conductance calculated for BDT came out to be 2 to 3 orders of magnitude higher than what was measured. The experiment done by Reed *et al*.[68] was done in a break junction setup but not using the statistical method of making a histogram. Soon after, a higher conductance of BDT (around 0.011 G_0) was reported experimentally[73] and was also found matching with theoretical results published by[70] where the electrodes were treated using a jellium model. A series of experiments studying BDT[73–79] and other molecules followed thereafter, using a variety of different statistical techniques (STMBJ, MCBJ etc.) both at room temperature and low temperature. A collection of some of these experiments on BDT is shown in Figure 1.4(a) with the measured conductance plotted against different techniques. The first experiment made by[68] is also included there.

Figure 1.4 (b) also shows the voltage at which the data points shown in the figure are measured. What we see is that although in some works[68,76] it is shown that the differential conductance increases with applied bias in a step manner, the different measurements tabulated in the Figure 1.4(b) don't follow any specific trend with bias.

[68] M. A. Reed et al. In: *Science* 278 (1997), p. 252.
[69] Eldon G. Emberly and George Kirczenow. In: *Phys. Rev. B* 58 (1998), p. 10911.
[70] M. Di Ventra et al. In: *Phys. Rev. Lett.* 84 (2000), p. 979.
[71] K. Stokbro et al. In: *Computational Materials Science* 27 (2003), p. 151.
[72] A. M. Bratkovsky and P. E. Kornilovitch. In: *Phys. Rev. B* 67 (2003), p. 115307.
[73] Xiao et al. In: *Nano Letters* 4 (2004), p. 267.
[74] Jochen Ulrich et al. In: *The Journal of Physical Chemistry B* 110 (2006), p. 2462.
[75] Makusu Tsutsui et al. In: *Applied Physics Letters* 89 (2006), p. 163111.
[76] Emanuel Lörtscher et al. In: *Phys. Rev. Lett.* 98 (2007), p. 176807.
[77] Wolfgang Haiss et al. In: *Journal of Physics: Condensed Matter* 20 (2008), p. 374119.
[78] Masateru Taniguchi et al. In: *Nanotechnology* 20 (2009), p. 434008.
[79] Youngsang Kim et al. In: *Nano Letters* 11 (2011), p. 3734.

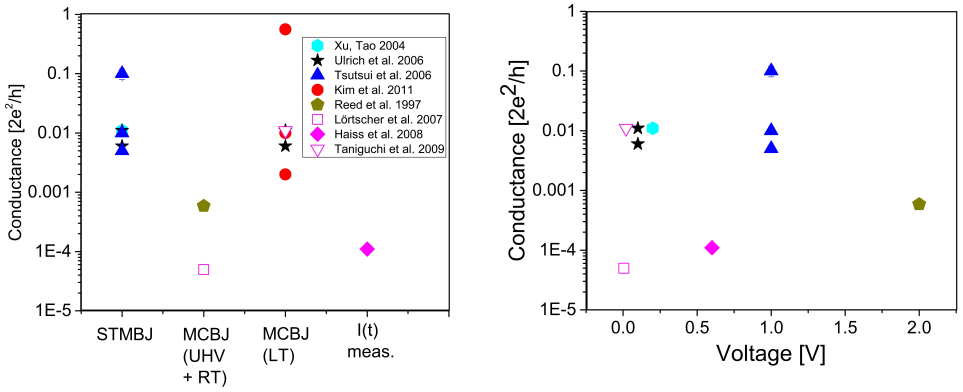

(a) (b)

Figure 1.4: (a) Spread of measured conductance values of BDT molecule with gold leads under different conditions (UHV, RT, LT) and different measurement techniques (STMBJ, MCBJ, I(t)). The different symbols signify different authors and the two unfilled symbols are the only ones measured at bias less than 50mV. (b) This graph shows the corresponding voltage bias at which the data points in (a) are measured.

The wide spread in the conductance of BDT was attributed to the different manner (orientation, contact site, nature of the bond etc.) the BDT could attach to the gold leads. The exact atomic structure of the gold electrode, the position of the Fermi level at the gold leads with respect to the HOMO and LUMO of the molecule, number and type of other molecules in the close vicinity (i.e., the environment of the molecule, presence of solvent molecules etc.) are also contributing to the spread. These uncertainties from the experiment side lead the theory to provide also a variety of different conductance (few mG_0 to 0.5 G_0[80]) values for BDT depending on the chosen position (orientation) of the molecule and the structure of the leads. Recent theoretical account of this is given elsewhere[81–84]. Also, a difference in the conductance gap is reported both among experiments[68,76] and among the theory[69,70].

Inelastic electron tunnelling spectroscopy (IETS)[5] measurements have also been reported[78,79] on the BDT molecule contacted between gold electrodes. Here the different vibration mode energies of the molecule have been shown to match with the theory presented in the individual article. The BDT junction over which these IETS measurements have been reported have conductance ranging from 0.002 to 0.5 G_0. Karimi *et al.*[85] have shown by doing shot-noise measurements, that electronic

[5] A discussion on it is given in Chapter 6

[80] Nikolai Sergueev et al. In: *Phys. Rev. B* 82 (2010), p. 073106.
[81] Mikkel Strange et al. In: *The Journal of Physical Chemistry Letters* 1 (2010), p. 1528.
[82] Renato Borges Pontes et al. In: *ACS Nano* 5 (2011), p. 795.
[83] William R. French et al. In: *The Journal of Physical Chemistry Letters* 4 (2013), p. 887.
[84] Amaury de Melo Souza et al. In: *Nanoscale* 6 (2014), p. 14495.
[85] M. A. Karimi et al. In: *Nano Letters* 16 (2016), p. 1803.

transport through BDT molecules takes place via a single channel over a wide range of conductance values (i. e. 0.01-0.24 G_0).

It has been reported recently[86] using transition voltage spectroscopy (TVS) that on stretching of the BDT molecule, the HOMO level which lies far below the Fermi level is pulled up towards it, giving rise to an increase in conductance due to resonance tunnelling. This increase can be up to few orders of magnitude. When the molecule is compressed (or titled) between the leads, there is again an increase in conductance due to increase in coupling of the π electrons in the benzene ring to the leads.

1.5.2 Alkane dithiols

Alkane dithiol (ADT) molecules coupled between two gold electrodes were the model system in the first decade of 21st century for single molecule electronics experiments. Before this period most of the electronic transport experiments in molecular electronics were mostly done on self assembled monolayers (SAM)[87] where 10s of molecules where contacted and measured. Cui *et al*.[88] were the first who have contacted and measured a single 1,8-octanedithiol (ADT8) molecule. They inserted a small concentration of ADT8 molecules in 1,8-octanethiol monolayer over a flat Au(111) surface. The octanethiol molecules acted as insulator and were used to separate single ADT8 molecules from one another. Now, on inserting this into a gold nano-particle solution, the dithiol molecules made a -SAu chemical bond with the nano-particles which were further probed using a conducting AFM tip. They reported conductance of around 1.43×10^{-5} G_0 at 0.1 V bias in Toulene solution environment. Later on the same group published data also for decanedithiol (ADT10) and dodecanedithiol (ADT12) and showed that the conductance of the ADT molecules decreases (with length of the molecule) exponentially with a decay constant β of 0.58 ± 0.06 per $-CH_2$ group. In 2003, Tao *et al*.[61,89] used an STM break junction method to probe hexanedithiol (ADT6), ADT8 and ADT10. They reported very different (almost one order of magnitude higher) conductance values than Cui *et al*.[88,90] at the same bias and a decay constant β of 1.04 ± 0.05 per $-CH_2$ group, which is similar to value a known for alkane thiols self-assembled mono-layers. Similar to Cui *et al*. , the measurements were also conducted in solution. The lower conductances measured in the previous work[88] was then speculated to be due to finite resistance between the AFM tip and the gold nano particle causing charging effects on the nanoparticle itself. Soon after in 2004 Haiss *et al*.[67] used the I(t) measurement technique to probe a similar set of molecules i.e., ADT6, ADT8 and nonanedithiol (ADT9). They found conductance values and a decay factor close to what was reported by Cui *et al*.[88,90]. After this, many groups measured different ADT molecules mainly using different versions of break junction techniques due to its simplicity, and also some I(t) and I(s) measurement.

A collection of the measured conductance values for different chain lengths of ADT molecules as obtained by single-molecule measurement techniques is collected in Figure 1.5. The conductance is placed on the y-axis in log scale, while x-axis is formed by the length of the ADT molecules in terms of the number of CH_2 groups

[86] Bruot Christopher et al. In: *Nature Nanotechnology* 7 (2011), p. 35.
[87] A. Salomon et al. In: *Advanced Materials* 15 (2003), p. 1881.
[88] X. D. Cui et al. In: *Science* 294 (2001), p. 571.
[89] Bingqian Xu et al. In: *Journal of the American Chemical Society* 125 (2003), p. 16164.
[90] X. D. Cui et al. In: *The Journal of Physical Chemistry B* 106 (2002), p. 8609.

in them. We see here orders of magnitude variation in conductance reported by different groups for each length of the molecule. Several groups have reported multiple conductance peaks, which are shown with different symbols in the Figure. We will discuss them in detail later. The two green ellipses define two regions of length of the molecules. For smaller length, the measured conductance is mostly constant, while for longer derivatives an exponential decay can be defined by fitting a straight line to the data. The slope of this fit, called the decay factor (or β) per CH_2, is measured by different groups. The inset of Figure 1.5 shows a histogram based on different β values recorded by different groups. A similar spread as shown in Figure 1.5 is also reported by Hihath *et al*.[91] while comparing the effects of different anchoring groups on the conductance values for alkane chains.

The orders of magnitude variations shown in the conductance measured for a simple family of alkane molecules questions our mastery of measuring and controlling electronic transport through single molecules. All the work done made us learn more about electronic transport through the molecule but also points towards our limited understanding of many aspects. We will go through a list of such aspects here.

The foremost one which is expected to be a major reason of variation in measured conductance is the lack of knowledge and control over the geometry of the contact between the molecule and the leads. It is seen from the limited number of configurations studied theoretically[111,112], that the conductance of the molecule can vary by more than an order of magnitude just based on the electrode configuration. In some later experiments it was also observed that there can be two[92–94,96,107] or even three[99,100,104] peaks in the histogram of conductance which are not integer multiples of the lowest conductance peak. Different characteristics conductance values observed in histograms for one molecule was attributed to the three possible combinations of binding sites for the sulphur(-S) atom on the gold leads. The -S atom can bind either to the hollow site between the gold atoms (which increases the conductance 'H') or on the top of the gold atom (which lowers conductance 'L'). Now three possible combinations are that (i) -S sits on an H-spot on both leads i.e., 'HH' or high conductance (HC) state, (ii) -S sits on both sides on an L-spot i.e., 'LL' or low conductance (LC) state and (iii) -S sits on one lead on an H spot and on the other lead on an L-spot i.e., 'LH' or 'HL' which is medium conductance (MC) state. These three conductance states were the most accepted explanation for the measured conductance peaks in the histogram. The probabilities (P) of these states occurring in the

[91] Joshua Hihath and Nongjian Tao. In: *Semiconductor Science and Technology* 29 (2014), p. 054007.
[111] K. H. Müller. In: *Phys. Rev. B* 73 (2006), p. 45403.
[112] John Tomfohr and Otto F. Sankey. In: *The Journal of Chemical Physics* 120 (2004), p. 1542.
[92] Jin He et al. In: *Faraday Discussion* 131 (2006), p. 145.
[93] Xiulan Li et al. In: *Journal of the American Chemical Society* 128 (2006), p. 2135.
[94] Fang Chen et al. In: *Journal of the American Chemical Society* 128 (2006), p. 15874.
[96] Emil Wierzbinski and Krzysztof Slowinski. In: *Langmuir* 22 (2006), p. 5205.
[107] Youngsang Kim et al. In: *Phys. Rev. Lett.* 106 (2011), p. 196804.
[99] Ayano Nishikawa et al. In: *Nanotechnology* 18 (2007), p. 424005.
[100] Chen Li et al. In: *Journal of the American Chemical Society* 130 (2008), p. 318.
[104] Wolfgang Haiss et al. In: *Phys. Chem. Chem. Phys.* 11 (2009), p. 10831.

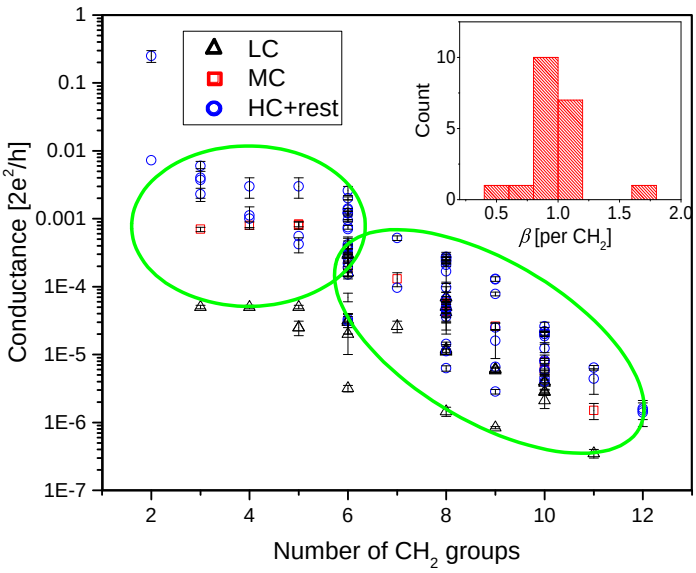

Figure 1.5: Spread of measured conductance values of ADT molecules vs their lengths in terms of number of $-CH_2$ groups in the backbone. The data is a collection of most of the published work[37,61,63–65,67,74,88,89,92–110] on ADT divided into four categories: low conductance (LC), medium conductance (MC), high conductance (HC) and 'rest' for the data not been classified by the respective authors in any of the three conductance states. Inset shows a histogram of reported[61,63,67,93–95,98,100,103–105,109,110] decay constants (β).

experiments were given as $P(LC) > P(MC) > P(HC)$, which was acceptable by the fact that the conductance of the molecule is measured while pulling the electrodes away from each other in break junction setup, which makes the -S atom sitting in the hollow site in both the gold electrodes under a tensile stress as least likely. It was also reported that other than these conductance states which depend only on the position of -S atom on Au electrodes, there could be more conductance states due to the conformation changes (trans or gauche)[99] of the molecule sitting in between the leads. Chen *et al*.[100] argued that many combinations of such contact geometries and conformations could coexist, which makes it difficult to even understand why in experiments one measures any peaks in the histogram. They explained on the basis of ab initio calculations, that the different junctions conformations are correlated and clustered together. This shows that one could expect peaks in the histogram but a single peak results from averaging over many junction configurations and does not point towards one favorable configuration. From the simulation Chen *et al*. also extract the information that the MC and HC configuration described above are due to all $trans$ conformers with atop-atop and bridge-bridge configuration respectively for S atom on Au leads. The LC configuration is supposedly originating form the

mixed *gauche* conformations which suggests that the LC series might not show pure exponential decay. This may explain why Haiss *et al*.[67] measured a smaller decay constant. Chen *et al*.[100] also provide an estimate that the combined effect of the uncertainty in contact geometry and conformation changes could give up to 2 orders of magnitude variation in conductance.

Irrespective of the large variation of the values of the measured conductance shown in Figure 1.5, it was reported repeatedly by many groups that there is an exponential decay of the conductance with length of the molecule. Although a varying set of decay constants have been reported as well, as shown in the inset of Figure 1.5, the exponential behavior suggests elastic tunneling or a superexchange process as the predominant electron transport mechanism for ADT molecules given by $G(N) = G(0)\exp(-\beta N)$. This length dependence appears to be followed for the larger length molecules ($N > 7$), as can be seen in Figure 1.5. The deviation from the exponential behavior for smaller length has been attributed to the fact that for smaller molecules the conductance could be more critically effected by the coupling of the chain through the sulphur groups[92].

It is experimentally also reported that the LC and HC conductance states for ADT8 are temperature independent between 269 to 315 K[93] and also from 4 to 40 K[108], while others show[113] for four different molecules from ADT family that the single molecule conductance are strongly dependent on temperature between 293 to 353 K. They attribute this to changes in the conformation of the molecule. The same group reports that this temperature dependence becomes suppressed as the molecules is squeezed or stretched not allowing the temperature induced conformation changes to take place[114].

Another question on the understanding of the formation of these molecular junctions is how does the molecule arrive between the electrodes? Huisman *et al*.[102] has provided an insight to this by pointing out the modified or enhanced plateau length of the Au-Au point contact plateau at 1 G_0 conductance. They have shown that in the presence of the molecules the 1 G_0 conductance plateau length is increased significantly, suggesting that the molecules already bridge the two electrodes before the first JOC is seen. With a simple spring model and taking the ratio of the length of the plateau with and without the molecules from the experiments they were able to show that the number of molecules that must be bridging the two electrodes were between 1 to 3. Dithiol molecules are in general also easy to polymerize due to oxidative disulfide formation and this could lead to contacting more than one molecule in series between the leads. Another aspect which is not known is the absence or presence of H atom in the sulphur gold bond i.e., -SAu (thiolate bond) or -SHAu (thiol bond). The occurrence of both the bonds is equally likely as both have similar binding energy, but it is known from theory that there can be around one order of magnitude variation in the conductance from one case to other[71], thiolate bond being more conducting. Most of the theory calculations done for dithiol molecules in order to compare with the experiments are done assuming thiolate bonds on both electrodes.

[108] Youngsang Kim et al. In: *ACS Nano* 5 (2011), p. 4104.
[113] Wolfgang Haiss et al. In: *Faraday Discuss.* 131 (2006), p. 253.
[114] Wolfgang Haiss et al. In: *Nature Materials* 6 (2006), p. 995.
[102] Everardus H. Huisman et al. In: *Nano Letters* 8 (2008), p. 3381.

The conductance histogram measured in the break junction experiments could also depend on the size of the Au-Au contact (junction conductance) formed upon indentation before separating the two electrodes and also on the speed of electrode separation. It has been reported that a maximum junction conductance of around 20 G_0 gives sharper peaks in the conductance[106]. Junction conductance from 0.2 G_0 (in tunneling) to 40 G_0 or higher have been reported. The need to make a sufficiently large junction was motivated by the idea of randomizing the tip structure and molecule coupling, giving more statistical parameter space to be explored. On the other hand the I(s) method proposed by Haiss *et al.* ,[67,104,114] and other non-contact experiments[95,100] have tried to minimize the variations coming from tip structure and avoid the strain due to jump out of contact on the breaking of gold atomic chain backbone. A systematic study of the effect of different indentation depth in break junction experiments to the non-contact case in I(s) type measurements in the single molecule conductance value and the FWHM of the histogram peak is missing from the literature. Another thing that is missing as mentioned earlier is the effect of different stretching rate or electrode speed on the conductance.

Some studies on the effect of the stretching rate on the length of the conductance plateaus have been done[97,115]. They have shown that for very slow (<4.4 nm/s) and very fast (>22 nm/s) stretching rate the stretching length remains independent of stretching rate but for the mid range the stretching length increases linearly with the logarithm of the stretching rate and this behavior is the same for molecular and metallic junctions. This further suggests that the final breakdown of the molecular junction might also be taking place at the Au-Au bond close to the metal molecule contact rather than at the Au-S bond. In fact, the stretching rate may also play a role on the measured conductance histogram of the molecule itself[65], as depending on the junction geometry and stretching rate it may be possible that the formation of Au-S chemical bond is getting effected[96] in the small millisecond time scale in which the measurement is performed and this could effect the conductance drastically.

Another interesting characteristics that has been seen in the single molecule conductance traces taken via break junction type techniques was a rise of conductance on stretching the molecule just before the breaking of the molecular junction. This type of increase contributes partly to the large spread in conductance histogram and so it is important to understand. Fujihira *et al.*[116] have pointed out that about 80% of the traces with molecules have this feature. One explanation to the increase was given in terms of transformation of the molecule conformation from $gauche$ to $trans$. A similar increase of conductance with stretching is also seen regularly in other molecules like benzenedithiol. Here the conductance increase is attributed to the shifting of HOMO related states close to the Fermi level during stretching[86] and the rise in conductance during stretching could even be up to one order of magnitude.

The effect of background in the statistical data is a problem in the analysis. When the measurements are done (specially break junction type), a large part of the traces have no signatures of the presence of a molecule, which gives after the Au contact

[106] C. A. Martin. PhD thesis. Kavli Institute of Nanoscience Delft, 2010.
[95] Slawomir Sek et al. In: *The Journal of Physical Chemistry B* 110 (2006), p. 19671.
[97] Huang et al. In: *Journal of the American Chemical Society* 129 (2007), p. 13225.
[115] Zhifeng Huang et al. In: *Nature Nanotechnology* 2 (2007), p. 698.
[116] Masamichi Fujihira et al. In: *Phys. Chem. Chem. Phys.* 8 (2006), p. 3876.

is broken a tunneling decay curve. The exact nature of the tunneling curve depends on the shape of the electrodes and the presence of local impurities (even the test molecules) on the two electrodes. These curves without molecules bridging the junction forms a large tunneling background in the histogram and could hide in it the useful features relevant to the molecules. In the previous section 1.4.4 on data analysis we have covered some common techniques to avoid such background effects. In an article by Rascon-Ramos *et al.*[110], the authors have shown that by adding an AC modulation to z motion of one of the electrode one could extract the mechanical properties of the contact and also get an idea of the most preferential binding site of S atom on Au leads. Such experiments help in reducing the unknowns and understanding to some extend the origin of the wide spread in the conductance histogram of molecules.

Using the examples of benzene dithiol and alkane dithiols, we discussed above the effects of different parameters on the measured conductance values and the limitations of the statistical measurement techniques. A better control of various input parameters can be achieved by moving towards single-shot measurements discussed in Part 1 of this thesis.

1.6 Shot noise

In addition to conductance, electronic transport through single molecules is also probed previously using shot-noise measurements. It is used mostly for determining the number of transmission channels involved in the electronic transport[85,117,118]. However, recently attempts have been made to use noise measurements also as a spectroscopic tool[119]. In this work, it is shown that there are signatures of electron-phonon interactions in usual noise spectra. Here, a gold metallic point contact is studied, and on exciting an electron-phonon vibration mode in gold (which is around 10-20mV), a linear kink in the noise spectra was recorded[120]. Figure 1.6 shows the result of such noise spectroscopy taken from the PhD Thesis of Manohar Kumar[119].

Shot noise occurs due to fluctuations in the number of electrons that are crossing a junction for an applied current or voltage bias. This fluctuation in electron number also exists for a macroscopic size contact. However, as the mean value of current can be very large, so these fluctuations are hardly visible. In nanocontacts, this fluctuation in the number of electrons passing through a cross-section gives a finite noise over the mean current. Moreover, in an independent electron system, the electron crossing time follows a statistical Poisson distribution. The noise generated by these fluctuations is called shot noise. An important difference between these fluctuations and thermal fluctuations is that the former will be present even at absolute zero temperature unlike the later. According to perturbation theory, the crossover from thermal noise (proportional to $k_B T$) to shot noise (proportional to eV) occurs at a voltage $eV = 2k_B T$. A correlation function P_{LR} for the fluctuations in current over the

[110] Habid Rascón-Ramos et al. In: *Nature Materials* 14 (2015), p. 517.
[117] D. Djukic and J. M. van Ruitenbeek. In: *Nano Letters* 6 (2006), p. 789.
[118] Regev Ben-Zvi et al. In: *ACS Nano* 7 (2013), p. 11147.
[119] Manohar Kumar. PhD thesis. Leiden Institute of Physics (LION), Leiden University, 2012.
[120] Manohar Kumar et al. In: *Phys. Rev. Lett.* 108 (2012), p. 146602.

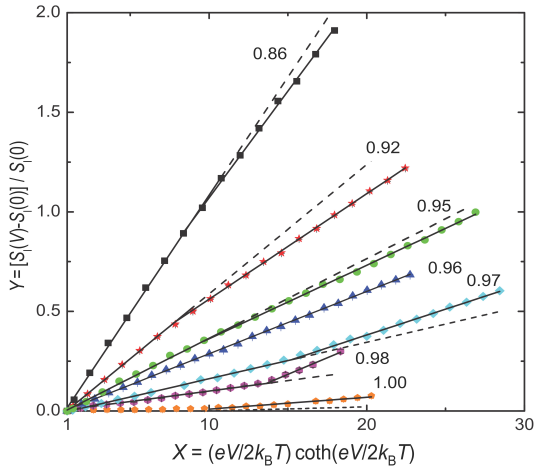

Figure 1.6: Kink in shot noise for a range of transmission values (from 0.86 to 1.00) of Au atomic chain: In this reduced axis plot the noise data below the vibron energy are described by a linear dependence (fitted with a solid line up to the kink, and extrapolated by a dashed line). Above the phonon energy, a new linear dependence is observed. Figure taken from the PhD Thesis of Manohar Kumar[119].

mean current (i. e. $\Delta\hat{I}_\alpha(t) = \hat{I}_\alpha(t) - \left\langle \hat{I}_\alpha \right\rangle$) in the left and the right leads can be written as –

$$P_{\mathrm{LR}}(t,t') = \frac{1}{2}\left\langle \Delta\hat{I}_{\mathrm{L}}(t)\Delta\hat{I}_{\mathrm{R}}(t') + \Delta\hat{I}_{\mathrm{R}}(t')\Delta\hat{I}_{\mathrm{L}}(t)\right\rangle \tag{1.4}$$

For stationary random fluctuations, i. e. for no time-dependent external fields, the noise power ($S_{LR}(\omega)$) associated with this correlation is directly given by its Fourier transform, which is also called Wiener-Khintchine theorem.

$$S_{\mathrm{LR}}(\omega) = \int_{-\infty}^{+\infty} \mathrm{d}\tau P_{\mathrm{LR}}(\tau = t - t')e^{-j\omega\tau} \tag{1.5}$$

In this thesis, we will use only the noise power or power spectral density ($S_{\mathrm{LR}}(\omega)$) and not the current correlation function ($P_{\mathrm{LR}}(t,t')$), as the former is the direct output from our FPGA based noise spectrum analyser as described in Chapter 4.

1.7 Two-level fluctuations

Two-level fluctuations are common in nanoscale junctions. They occur due to stochastic fluctuations of an atomic or molecular junction between two stable conductance states. These fluctuations are measured by bringing an STM tip above a molecule adsorbed on a surface[121] and also for molecular and atomic junctions formed using mechanically controlled break junction[122,123]. Figure 1.7(a) is a schematic depiction

[121] N. Néel et al. In: *Nano Letters* 11 (2011), p. 3593.
[122] Alexei Marchenkov et al. In: *Phys. Rev. Lett.* 98 (2007), p. 046802.
[123] W. H. A. Thijssen et al. In: *New Journal of Physics* 10 (2008), p. 033005.

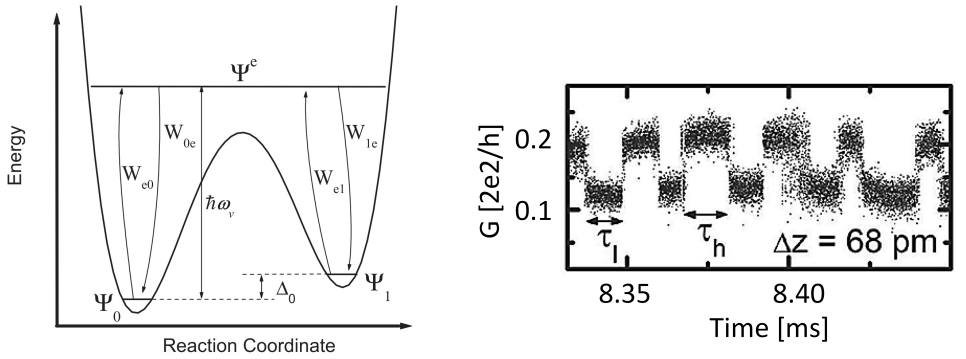

(a) (b)

Figure 1.7: (a) An energy diagram of a two level system taken from Thijssen *et al.*[124]. It shows the reaction kinetics involved in transfer of energy from a molecular vibration to excitement to a different conductance state. (b) Conductance fluctuation measured over a C_{60} molecule[121] once an STM tip is brought towards it.

(taken from Thijssen *et al.*[124]) of such bistable conductance states separated by a small energy barrier. It has been shown[124] that these two-level fluctuations can also be induced by an electron-phonon interaction, which could provide sufficient energy to cross the barrier. This process takes place along a certain reaction coordinate. Persson and Ueba[125] have shown that similar inelastic interaction can be used to move molecules over a metallic surface using STM tip.

Figure 1.7(b) shows a conductance fluctuation example taken from Néel *et al.*[121], where a two-level fluctuation is seen over a C_{60} molecule once an STM tip is brought towards it. This is a typical example of a two-level fluctuation, where two different conductance states occur with different mean residence times for the high (τ_1) and low state (τ_2). The power spectral density for the noise generated by such two-level fluctuations is Lorentzian in shape and is given by –

$$S_{2L}(\omega) = 4\Delta R^2 \frac{{\tau_{\text{eff}}}^2}{\tau_1 + \tau_2} \frac{1}{1 + \omega^2 {\tau_{\text{eff}}}^2} \tag{1.6}$$

here, $\frac{1}{\tau_{\text{eff}}} = \frac{1}{\tau_1} + \frac{1}{\tau_2}$ and ΔR is difference in the resistance values of the two states.

1.8 Organization of the thesis

More than three decades have passed since the first single-molecule experiment was performed by Reed *et al.*[68]. The main techniques that are used to study single-molecule transport to date do not provide many crucial pieces of information about the system. Most important are the atomic structure of the contacting leads and the binding configuration of the molecule.

There are three main questions that this thesis is aiming to answer –

[124] W. H. A. Thijssen et al. In: *Phys. Rev. Lett.* 97 (2006), p. 226806.
[125] B. N. J. Persson and H. Ueba. In: *Surface Science* 502-503 (2002), p. 18.

The first question that this thesis is going to answer is how can we make the single-molecule transport measurements more controlled? What extra information can we obtain from these measurements to bridge the gap between experiments and theory? These questions will be the subject of Part 1 of the thesis. Here we prepare a benchmark single-molecule test setup for single-shot measurements.

The second question that we are aiming at is, can we do more with shot-noise measurement? Shot noise is the second cumulant of current while conductance is the first. Thus shot noise is more sensitive to electron-electron and electron-phonon interactions. In spite of that, most of the shot-noise measurements done on single-molecules and atomic junctions have aimed at low energy regime to mainly obtain the information about the number of channels involved in the transport. Recently, it has been shown that shot noise can also be used to probe inelastic electron-phonon interactions in Au metallic contacts. However, no measurements have been done on probing such interactions in single molecules. In Part 2 of the thesis, we will study shot noise at high bias probing single atomic point contacts in non-linear regime and single molecules.

Third and the last question that we also worked on is related to the use of graphene-based electrodes in molecular electronics. Graphene offers a unique platform to study single-molecules. The two-dimensional structure of this material offers the flexibility to image the contacts atomic structure and molecules binding configurations. To this end, we need to have atomic-scale control of the nanogaps formation in graphene. The commonly used electroburning technique does not provide such a control. Thus, in Part 3 of this thesis, we will explore other techniques to make controlled nanogaps in graphene.